

**UNIVERSITY OF SÃO PAULO  
INSTITUTE OF ASTRONOMY, GEOPHYSICS, AND ATMOSPHERIC SCIENCES  
DEPARTMENT OF ATMOSPHERIC SCIENCES**



**AIR-SEA INTERACTION LABORATORY  
MICROMETEOROLOGY GROUP**

**MASTER QUALIFYING EXAMINATION**

**VERTICAL TURBULENT FLUXES OF HEAT AND MOMENTUM IN THE  
ANTARCTIC REGION**

**Student: Marco Aurélio Alvarenga Alves**

**Supervisor: Jacyra Soares**

São Paulo  
2015

## ABSTRACT

The Antarctic region is one of the untouchable places by the human society and, at the same time, susceptible to the climatic variations. Global numerical weather prediction and climate models require information about atmospheric conditions in Antarctic region to be used as input on these models through parameterizations, which help to describe the weather in that region and predict the weather in other regions on the planet. This work proposes to study the vertical turbulent fluxes of heat and momentum in the Antarctic region, more specifically in the Antarctica Brazilian Station – Estação Comandante Ferraz (EACF - 62°05'07" S, 58°23'33" W), located in King George Island. The purpose consisted in to obtain indirectly the vertical turbulent fluxes of heat and momentum utilizing the Monin-Obukhov Similarity Theory. A Fortran 90 algorithmic was used, for data of January 2014. The internal parameters (characteristic scales and Obukhov length) presented variation agreeing with the observed atmospheric conditions. The preliminary results showed the diurnal variation of turbulent heat fluxes (latent and sensible), with positive values during this month characterized predominantly by the stability parameter as an unstable period. Most of sensible and latent heat flux values were around 0 and 50 Wm<sup>-2</sup>, respectively. The momentum flux presented most of the values between 0 and 0.1 Nm<sup>-2</sup> and the peaks around 1 ms<sup>-1</sup> were associated to intense winds due to cyclone passage over the region. Sometimes, the wind velocity has a non-logarithmic vertical profile, and the air observed in the middle level (5.25 m) is colder and dryer than the other investigated levels.

**Key words:** Turbulent sensible heat flux, turbulent latent heat flux, momentum flux, Monin-Obukhov similarity theory, Antarctic region.

## 1. INTRODUCTION

The Antarctica region is one of the most preserved and most vulnerable place on the planet to environmental changes. Therefore, alterations in this environment, natural or anthropogenic, have a potential to biologic and socioeconomic impacts, which may affect the Earth system as a whole (Laws, 1990). The atmospheric system monitoring is essential to evaluate these changes, which means collecting continuously environmental data, with quality and for a long period, contributing in assessment of future implications, subsidizing decision-making.

A way of assessing the atmospheric conditions in Antarctica is through the study of the Planetary Boundary Layer (PBL) in the region. The PBL is the turbulent atmosphere adjacent to the surface, where is located most of human activities and its properties are determined by the thermal and dynamical effects of surface (Stull 1988).

The PBL has its origin linked to the exchanges of energy, momentum, and mass between the atmosphere and the surface, modulated by the turbulence on time scale of around one hour. In this time scale, the sensible and latent heat vertical turbulent fluxes determine the vertical mean structure of temperature and moisture in the PBL, while the vertical turbulent flux of horizontal momentum gives condition to the dynamic mean structure of the PBL, both on continental and oceanic regions in high and lower latitudes (Stull 1988; Arya 2005).

The vertical turbulent fluxes may be estimated directly from the covariance method. The covariance is estimated between the statistical fluctuations of vertical velocity wind and the respective variables (specific humidity of air for the latent heat flux and air temperature for the sensible heat flux). This method requires measurements of these fluctuations with a sample of at least 1 Hz (WGASF 2000; Arya 2005).

An alternative way of estimating the surface layer fluxes is indirectly, through observations of air specific humidity, air temperature and horizontal wind velocity by the Monin-Obukhov Similarity Theory (MOST). This indirect method requires observation of these properties at least three level of height and time average values of the variable of ten minutes to one hour (Stull 1988).

The goal of this study is to provide an estimative of the surface layer fluxes by the indirect form in the Antarctic Brazilian Station – Estação Antártica Comandante Ferraz (EACF), located in King George Island.

The data used in this work was obtained by the ETA Project (financial support by CNPq) and of INCT-APA.

### **1.1. Objectives**

The general objective of this work is to estimate the vertical turbulent fluxes of heat and momentum - through the indirect method - in the atmospheric surface layer of the EACF, using the Monin–Obukhov similarity theory.

In the future it will be performed the comparison of the turbulent fluxes estimated indirectly and by the direct form. In addition, the simultaneous information of the turbulent fluxes and the observation about the vertical gradient of temperature, humidity and velocity wind will allow the validation and calibration of the parameterizations utilized in atmospheric numerical models.

## **2. INVESTIGATED REGION AND DATASET**

The Antarctic Brazilian Station – EACF – is located in Keller Peninsula, into the Bay Admiralty, King George Island, in South Shetland Islands, in Antarctic Peninsula ( $62^{\circ}05'07''$  S,  $58^{\circ}23'33''$  W, 20 m about mean sea level). The islands are situated to 130 km of the Antarctic continent and to 849 km of the southernmost point of the South American continent – Cape Horn (Fig. 1).

According to Jones and Simmonds (1993), low-pressure centres moving toward the east in the circumpolar west wind zone of Southern Hemisphere dominate the climatic conditions in King George Island.

The geographical position of the Island leads to a polar maritime climate, especially for lower elevations as where EACF is located. The temperature is relatively warm (temperature rising above  $0^{\circ}\text{C}$  during summer), with a small variability in the mean annual temperatures, snow melt starting usually in November and lasting until March (2/3 for the energy available for melt comes from the net radiation) (Bintanja 1995; Smith et al. 1996; and Wen et al. 1998).

Cold and dry air masses occasionally may be advected toward King George Island due to barrier winds along the east coast of the Antarctic Peninsula, which often persists for 1 day or more (Schwerdtfeger 1984). By the other hand, the passage of warm and humid air masses from the northerly directions, associated to cyclonic systems along the northern Antarctic Peninsula is responsible for the melt events in the Island (Braun et al. 2001).

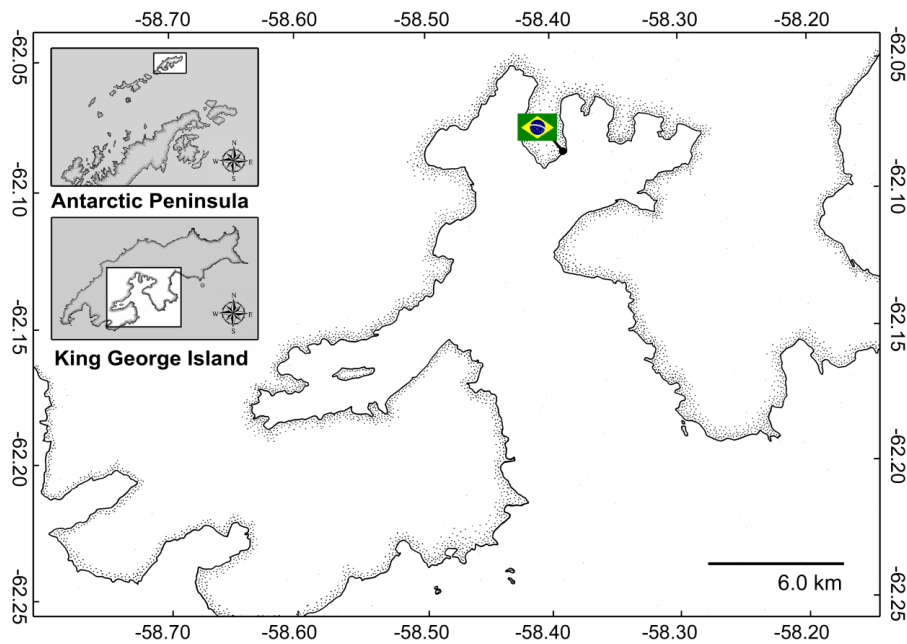


**Figure 1:** Geographic location of the Brazilian Antarctic Station in the King George Island. Adapted from Moura (2009).

The data used in this study was obtained, by the ETA Project, during January of 2014, in the EACF.

It was used *in situ* observations of the wind velocity and direction, air temperature, and air relative humidity, in three different levels of height, installed in a micrometeorological tower of 12 m (Fig. 2). The sampling frequency was of 10 Hz stored as 5 min average by a data-logger (CR5000, Campbell Scientific Inc.) using the local time (-4 UTC) as standard time. Pressure values, at 1.35 m of height, were also used. The sensor specifications and respective height are described in Table 1.

The instruments installed at the tower are connected to a datalogger, which is also connected to a laptop inside the Meteorology laboratory and transmits the data instantly to the Air-Sea Interaction Laboratory in IAG/USP.

**Table 1: Sensor specifications**

Sensor	Variable	Range	Accuracy	Height (m)
RM Young Model 05103 <sup>1</sup>	Wind velocity	0-100 ms <sup>-1</sup>	±0.3 ms <sup>-1</sup>	2.1 (Level 1) 5.15 (Level 2) 10.2 (Level 3)
	Wind direction	0-360°	± 3°	
Campbell Sci. Model CS215 <sup>2</sup>	Air temperature	-40°C to +70°C	±0.3°C at 25°C ±0.4°C (+5°C to +40°C) ±0.9° (-40° to +70°C)	2.2 (Level 1) 5.25 (Level 2) 10.3 (level 3)
	Air relative humidity	0 to 100%	±2% (10% to 90%) ±4% (0% to 100%)	
Vaisala PTB110 <sup>3</sup>	Pressure	Several pressure ranges	±0.3 hPa at +20°C	1.35

<sup>1</sup> available in: <http://www.youngusa.com/products/7/5.html>

<sup>2</sup> available in: <https://www.campbellsci.com/cs215-specifications>

<sup>3</sup> available in: <http://www.vaisala.com/en/industrialmeasurements/products/barometricpressure/Pages/PTB110.aspx>

The micrometeorological tower was installed over a region with different surface characteristics. At the North of the tower there is the Stenhouse glacier; at South, the Admiralty Bay, comprehend by the Martel Inlet and some bare soil; at East side there is the Admiralty Bay and at West side there is bare soil, represented by hills, as illustrated in Figure 2.

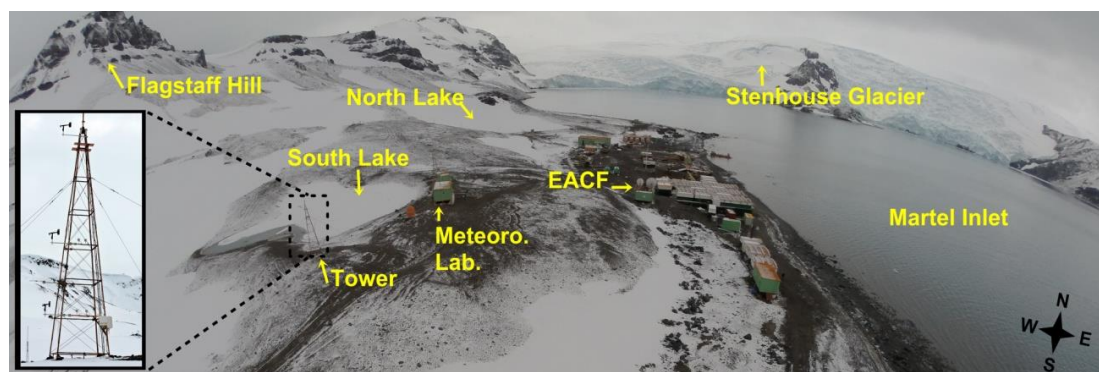


**Figure 2:** Aerial view from the Micrometeorological tower (photography copyright Renato Torlay).

### 3. METEOROLOGICAL CHARACTERISTICS DURING THE INVESTIGATED PERIOD

During January 2014, the wind velocity reached its maximum value of 22.3 ms<sup>-1</sup> at year day 12. The wind velocity monthly averaged was about 4.9 ms<sup>-1</sup>. The highest value of atmospheric pressure was 1004.2 hPa during day 09 and

the lowest value of 976.4 hPa during day 26 (Fig. 3a). It may be observed that during low-pressure conditions, the wind velocity is stronger than during the presence of high-pressure systems, and, there is no clear relationship with the wind direction (Figs. 3).

The periods over systems of high pressure with wind direction from E-SE have also been the periods with the lowest values of temperature, which agrees with the result presented by Kejna (1993) apud Braun et al. (2004). The author has studied synoptic maps, in the King George area, from 1986 to 1989. It was distinguished 21 circulation types, using pressure centre type and air mass transport as major parameters of classification. According with his study, a system of high-pressure acting on Antarctic Peninsula causes advection of cold air masses from E-SE due to the barrier winds. Besides that, an anticyclone centre over the northern Weddell Sea is the responsible for winds from N-NE, while winds from S are associated to anticyclones over the southern of the Antarctic Peninsula. When high-pressure systems are situated in the North of the King George Island, the mass transports are leading for winds coming from West quadrant (SW, W and NW). By the other hand, over low-pressure systems (in general, approaches its centre toward the West of the King George Island over the Bellingshausen Sea) it can be seen winds coming from N and NW, while cyclones over the Drake Passage are associated to winds from E and NE.

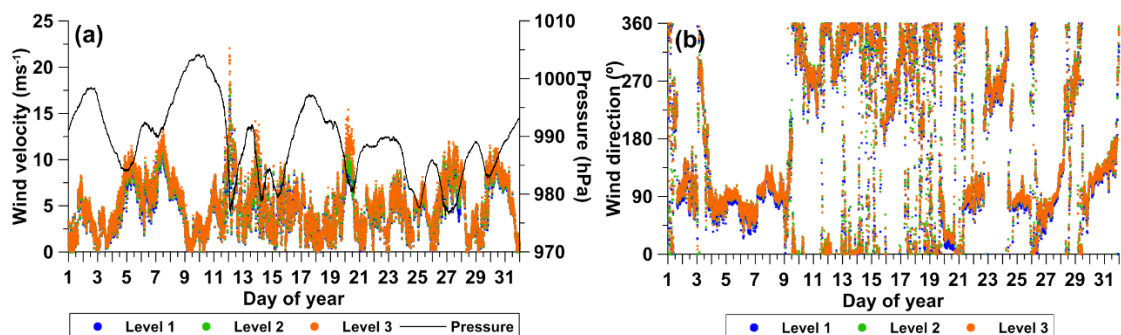


**Figure 3:** Temporal variation of (a) wind velocity ( $\text{ms}^{-1}$ ) and atmospheric pressure (black line, in hPa) and (b) wind direction (degree), for January 2014. Blue, green and orange points represent the values obtained at level 1, 2 and 3, respectively. The data sampling was 10 Hz and it was stored as 5-min average.

The preferential wind direction for this month was from East with high values of velocity between 10 and 20  $\text{ms}^{-1}$  (Fig. 4). Easterly winds coming from Weddell Sea area are responsible for temperature drops in the King George

Island region, as discussed by Parish (1983) and Schwerdtfeger (1984). Easterly winds are usually associated with westward-moving cold, stable air masses in the lowest 1,500 m of the atmosphere, reaching the mountain barrier of Antarctica Peninsula and deflected to the North (the barrier winds).

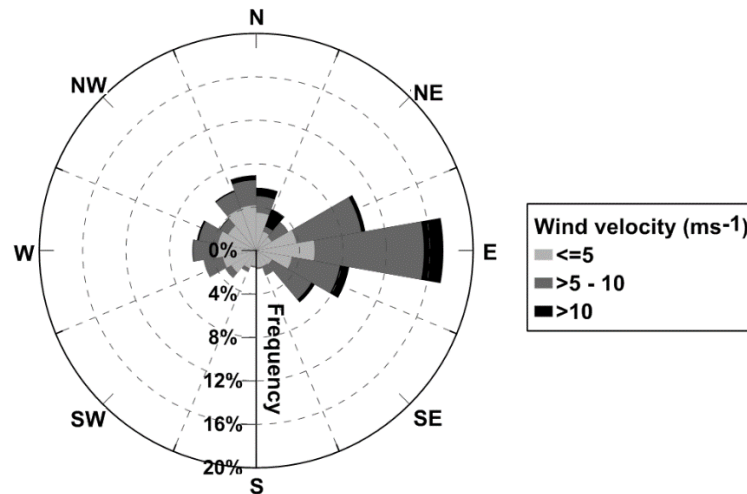


**Figure 4:** Distribution of wind velocity frequency related to the wind direction, measure at 10.2 m (third level) during January 2014. The data sampling was 10 Hz and it was stored as 5-min average.

The lowest air temperature recorded near the surface (height of 2.1 m), during January was around  $-3.5\text{ }^{\circ}\text{C}$  (with weak winds from the northern) during day 09 and the highest around  $7.0\text{ }^{\circ}\text{C}$ , during day 13 (over wind velocity around  $10\text{ m s}^{-1}$  from North-West), as seen in Fig. 5a. The air temperature monthly averaged, near the surface, was about  $0.6\text{ }^{\circ}\text{C}$ , what agrees with previous studies. Rachlewicz (1997) and Rakusa-Suszczewski (1993) have shown that the average monthly air temperatures during summer periods reaches values above  $0\text{ }^{\circ}\text{C}$ . It also can happen during winter periods, near the coast, due to the advection of warm humid air masses.

The air specific humidity presented its minimum value of  $1.91\text{ gkg}^{-1}$  in 09 January and maximum of  $5.26\text{ gkg}^{-1}$  during day 13 (Fig. 5b), with monthly average of  $3.27\text{ gkg}^{-1}$ , which correspond respectively to the periods of lower and higher values of temperature. According to Bintanja (1995), during summer, it is usual to observe temperature values above  $0^{\circ}\text{C}$  in the Brazilian Station due to the occurrence of Föhn-type winds coming from the Northern side of the Station,



which advect warm and dry air, rising the temperature in this region compared to the Northwest side (Martianov and Rakusa-Suszczewski 1989).

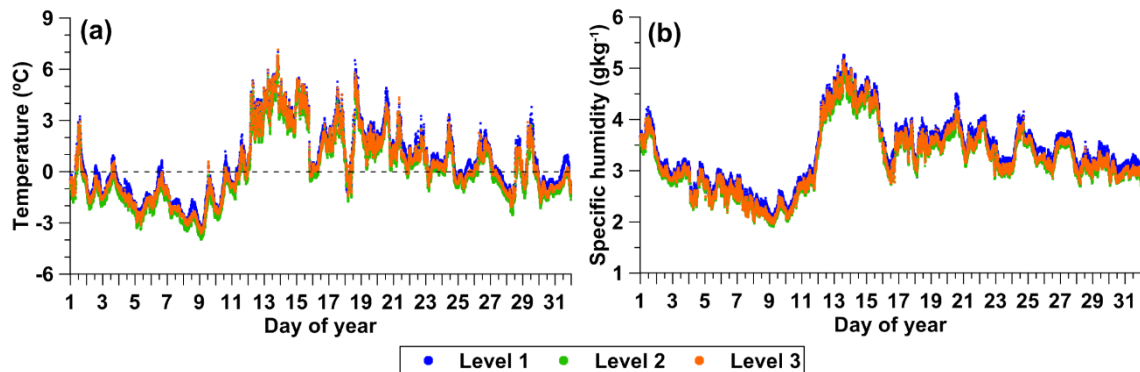


**Figure 5:** Temporal variation of (a) air temperature (°C). The horizontal dashed line indicates 0 °C and (b) air specific humidity ( $\text{gkg}^{-1}$ ) for January 2014. Blue, green and orange points represent the values obtained at level 1, 2 and 3, respectively. The data sampling was 10 Hz and it was stored as 5-min average.

The vertical profile measurements for the whole January 2014, revealed some interesting characteristics in that region. The measurements of air temperature and specific humidity presented most of the investigated time, a colder and dry air in the middle level (5.25 m of height) of measurement, as illustrated in Figure 6.

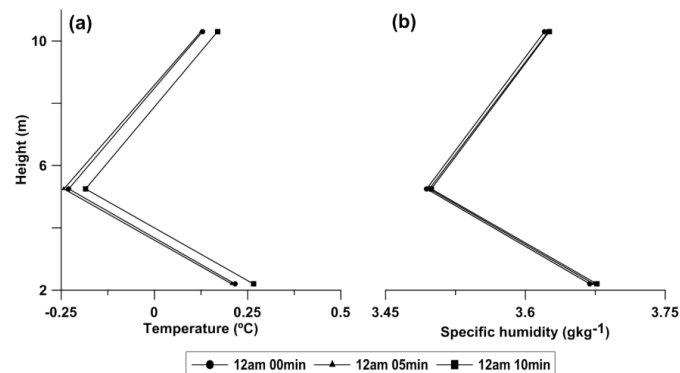


**Figure 6:** Vertical profile of (a) air temperature and (b) air specific humidity in 1<sup>st</sup> January 2014 at 12h00, 12h05 and 12h10. The data sampling was 10 Hz and it was stored as 5-min average.

#### 4. ESTIMATIVE OF THE VERTICAL TURBULENT FLUXES

Here, the estimative of the vertical turbulent fluxes were performed using the indirect method and the data described in Table 1. The data sampling utilized was 10 Hz and it was stored as 5 min average.

## 4.1 Flux-Profile Relationship

The vertical turbulent fluxes were estimated indirectly using the MOST. A Fortran 90 algorithmic of the Air-Sea Interaction Laboratory of the Micrometeorology Group of the IAG/USP was used to obtain the turbulent fluxes in the surface layer (SL). The surface layer is the first layer in the PBL, adjacent to the surface, and corresponds for one tenth of the PBL, where the turbulent fluxes are considered as non-divergent and approximately constants (Monin and Obukhov 1954; Dyer 1974).

The flux-profile relationship in the SL might be estimate by the MOST, considering the surface layer as horizontally homogeneous and stationary, which is useful when direct method of turbulent fluxes are not available (Arya 2001). The theory proposes local similarity functions (universal functions) for momentum ( $\Phi_m$ ) and heat/humidity ( $\Phi_{H,q}$ ), which are unique for each type of atmospheric conditions.

For atmospheric neutral and unstable conditions, the functions have shown good results when compared with the direct method (Businger et al. 1971; Hicks 1976; Högström 1988). For a stable atmosphere, especially over weak winds condition (strong stratification); the comparison with the direct method has not provided good agreement (Lee 1997, Sharan et al. 2003). The restrictions are due to weak and intermittent turbulence, presence of internal waves, Kelvin-Helmholtz instabilities, etc (Finnigan et al. 1984; Mahrt 1989; Yagüe and Cano 1994; Mahrt et al. 1998; Cuxart et al. 2000; Poulos et al. 2002). Therefore, different researchers have proposed improvements to the method (Zilitinkevich and Chailikov 1968; Webb 1970; Businger et al. 1971; Dyer 1974; Hicks 1976; Högström 1996, Zilitinkevich et al. 2007, Zilitinkevich and Esau 2007).

The flux-profile method was described by Dyer (1965, 1967, 1968 and, 1974), Businger et al. (1971), Yagüe et al. (2006), Kramm et al. (2013) among others. The method is iterative and introduces dimensionless gradients of the average variables of horizontal wind velocity ( $\bar{u}$ ), air potential temperature ( $\bar{\theta}$ ) and air specific humidity ( $\bar{q}$ ) into universal functions related to the stability parameter ( $\zeta = z/L$ ), which is a ratio between the height ( $z$ ) and Obukhov length ( $L$ ) at the reference level (Monin and Obukhov 1954). In unstable stratification,

the parameter is negative and positive for stable stratification. Values around zero mean neutral stratification.

The height ( $z$ ) is given by the difference between the height of measurement ( $h$ ) and the displacement height ( $d$ ), as following:

$$z = h - d \quad (1)$$

For  $z > L$  the buoyancy influence is the dominant factor (Yagüe et al. 2006). The  $|L|$  is the height above the ground where the buoyancy and shear production of turbulent kinetic energy are of equal magnitude; below this height shear dominates and above it, buoyancy dominates.

The  $L$  expression is given by (Kramm et al. 2013):

$$L = \frac{u_*^2}{\kappa \frac{g}{\theta_0} (\theta_* + 0.00061 \theta_0 q_*)} \quad (2)$$

where  $u_*$  is the scale of horizontal velocity,  $\kappa$  is the Von Kármán constant defined here as 0.4,  $\theta_*$  is the scale of temperature,  $\theta_0$  is the reference potential temperature, and  $q_*$  is the scale of specific humidity .

The average variables for  $\bar{u}$ ,  $\bar{\theta}$  and  $\bar{q}$  are given by (Kramm et al. 2013) as:

$$\bar{u}(z) = \frac{u_*}{\kappa} \left\{ \ln \left( \frac{z}{z_0} \right) - \psi_M(\zeta_0, \zeta) \right\} \quad (3)$$

$$\bar{\theta}(z) = \theta_0 + \frac{\theta_*}{\kappa} \left\{ \ln \left( \frac{z}{z_0} \right) - \psi_{H,q}(\zeta_0, \zeta) \right\} \quad (4)$$

$$\bar{q}(z) = q_0 + \frac{q_*}{\kappa} \left\{ \ln \left( \frac{z}{z_0} \right) - \psi_{H,q}(\zeta_0, \zeta) \right\} \quad (5)$$

where  $z_0$  is the roughness length,  $q_0$  is the reference air specific humidity.  $\psi_M$  and  $\psi_{H,q}$  are the universal functions related to stability parameter at an initial time to a posterior time ( $\zeta_t \rightarrow \zeta_{t+1}$ ), improving the corrections about the atmospheric conditions. The correction functions ( $\psi_M, \psi_{H,q}$ ) are given integrating the expressions with the stability parameters as limits. Thus, the integrated functions given by Paulson (1970) for unstable situations are:

$$\psi_M = 2 \ln \left[ \frac{(1 + \Phi_M)}{2} \right] + \ln \left[ \frac{(1 + \Phi_M^2)}{2} \right] - 2 \tan^{-1}(\Phi_M) + \frac{\pi}{2} \quad (6)$$

$$\psi_{H,q} = 2 \ln \left[ \frac{(1 + \Phi_{H,q}^2)}{2} \right] \quad (7)$$

where  $\Phi_M$  and  $\Phi_{H,q}$  are the dimensionless gradients of momentum and heat/humidity respectively and are given by (Paulson 1970):

$$\Phi_M = (1 - \gamma_1 \zeta)^{1/4} \quad (8)$$

$$\Phi_{H,q} = (1 - \gamma_2 \zeta)^{1/2} \quad (9)$$

here  $\gamma_1$  and  $\gamma_2$  are constants, which as suggested by Dyer (1974) and Hicks (1976) are both equal to 15.

For stable conditions, it follows, the expression (10) suggested by Webb (1970):

$$\psi_M = \psi_{H,q} = -\beta_{(M,H,q)} \frac{z}{L} \quad (10)$$

where  $\beta_{(M,H,q)}$  is a constant value for momentum and heat/humidity suggested by Webb (1970) as 0.5.

The method initially assumes neutral condition ( $\zeta^0 = \zeta_0^0 = 0$ ) for the atmosphere. After this consideration, a straight-line equation ( $y = \alpha + \beta x$ ) is adjusting to the measurement levels (three levels of observation) by the method of least squares. The first scale characteristics ( $u_*$ ,  $\theta_*$ , and  $q_*$ ) are found by the angular coefficient of the straight-line equation and then the universal functions can be estimated.

The scale characteristics of momentum, heat and humidity and the roughness length are given by:

$$u_* = \beta_u \kappa, \quad \theta_* = \beta_\theta \kappa / \mu, \quad q_* = \beta_q \kappa / \mu, \quad z_0 = \exp(\alpha_u)$$

where  $\beta_u$ ,  $\beta_\theta$  and  $\beta_q$  are the angular coefficient for the scale characteristic of horizontal wind velocity, temperature and humidity,  $\mu$  (equal to 1) is a constant value and  $\alpha_u$  is the straight line coefficient of the horizontal wind velocity.

Given the characteristic scales, the vertical of sensible (H) and latent (LE) turbulent heat fluxes and momentum ( $\tau$ ) can be expressed as (Fairall et al. 1996):

$$H = -\rho_0 c_p u_* \theta_* \quad (11)$$

$$LE = -\rho_0 L_V u_* q_* \quad (12)$$

$$\tau = \rho_0 (u_*)^2 \quad (13)$$

where  $\rho_0$  is the air density ( $1.15 \text{ kgm}^{-3}$ ),  $c_p$  is the specific heat of dry air at constant pressure ( $1004 \text{ J K}^{-1}\text{kg}^{-1}$ ) and  $L_V$  is the latent heat of vaporization ( $2,500 \text{ Jg}^{-1}$ ).

The energy balance components are considered here positive when the fluxes are from surface toward the atmosphere.

## 5. INITIAL RESULTS AND DISCUSSION

The results obtained utilizing the indirect method to estimate the vertical turbulent fluxes of heat and momentum are discussed below.

Characteristic scales ( $u_*$ ,  $\theta_*$ , and  $q_*$ ) (Fig. 7) have agreed with theory, which suggest that these scales are the measure of the mean vertical gradient (here estimated by the method of least square) corrected by the stability parameter (Businger et al. 1971).

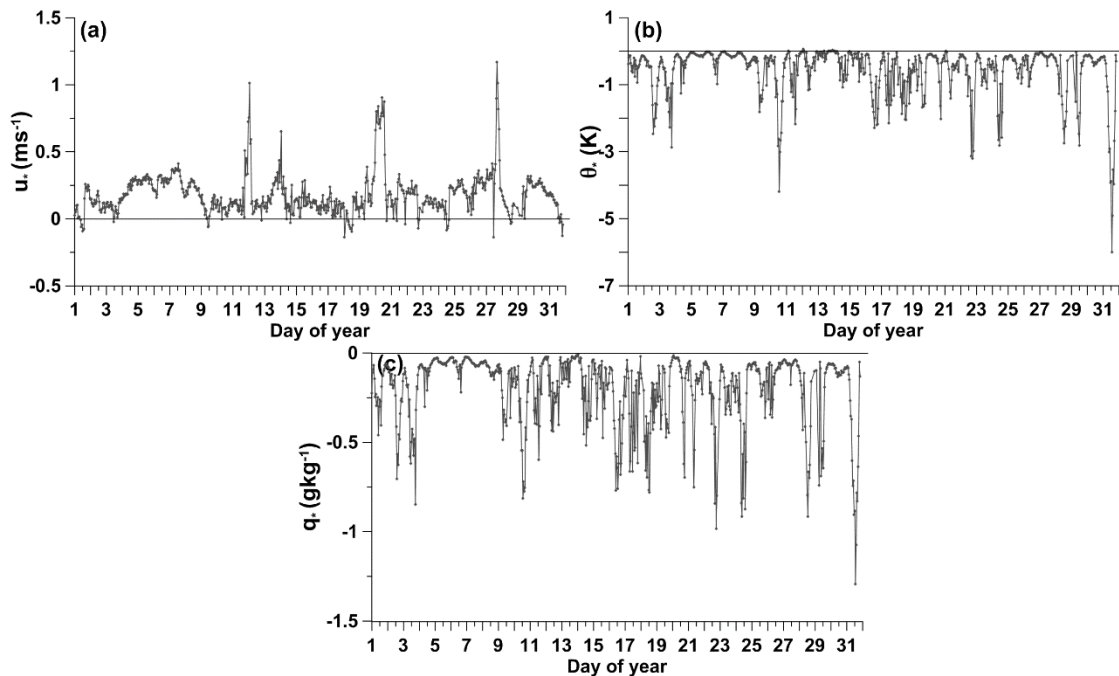


**Figure 7:** Temporal variation of the hourly averaged values of scale characteristics of (a) velocity, (b) air temperature and (c) air specific humidity during January 2014 (horizontal straight line indicates 0 value).

Most of the characteristic scale of velocity values are between 0 and 0.3  $\text{ms}^{-1}$  (Fig.8a) in agreement with Stull (1988), and peaks with maximum value above 1.0  $\text{ms}^{-1}$  (Fig.7a). These peaks were observed particularly during the night over intense winds coming from N and E, influenced in large scale by low-pressure centres (Fig.3a), during transition periods (Fig.9a). Negative values of this characteristic scale were also observed, and it is related to intense winds in the lower level of observation, representing less than 5% of values (Figs. 8a).

Characteristic scales of potential temperature and humidity show a diurnal variation with values higher during the day (Fig. 7b, c), related to diurnal heating of surface, responsible for larger vertical gradient of these variables. During January, most of the values of  $\theta_*$  varied between 0 and -0.5 K, and  $q_*$  varied between 0 and -0.2  $\text{gkg}^{-1}$ . From day 04 to 09 is noted small variation of these scales with negative values around zero, influenced by the advection of a cold and dry air mass originated of a high-pressure centre located over the Antarctic Peninsula and Weddell Sea (east of Antarctic Peninsula) with winds from E. This air mass has favoured the vertical homogenization of thermodynamic properties in the measurement level.

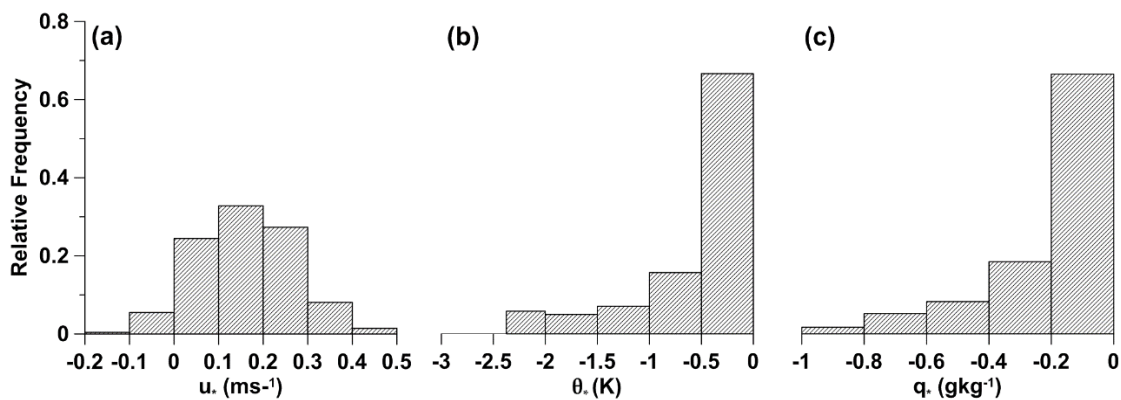


**Figure 8:** Histogram of the hourly averaged characteristic scales of (a) velocity, (b) potential temperature ( $\theta_*$ ), and (c) humidity for January 2014.

During the investigated period, the Obukhov length ( $L$ ) mostly indicates an unstable atmosphere (Fig.9). Stable periods were observed in a few days, especially at night, agreeing with negative values of  $H$  (Fig.10a).

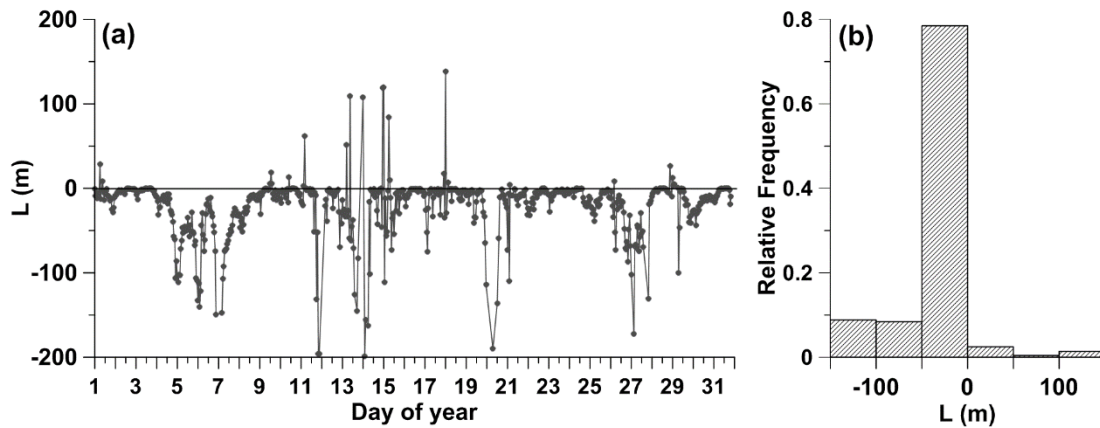


**Figure 9:** Temporal variation of the hourly averaged values of (a) Obukhov length ( $L$ ) (horizontal straight line indicates 0 value) and (b) histogram of  $L$  during January 2014.

The  $H$  presented a diurnal cycle (Fig. 10a), with higher values during the day and lower at night.  $H$  is 75% comprehended in a range of 0 - 100  $\text{Wm}^{-2}$ , with most of values smaller than 50  $\text{Wm}^{-2}$  (Fig. 11a), which may be related to the time of sunlight (approximately 18h30min of sunlight) and consequently to a larger heating of the surface. The negative values of  $H$  correspond to less than 10% of the data.

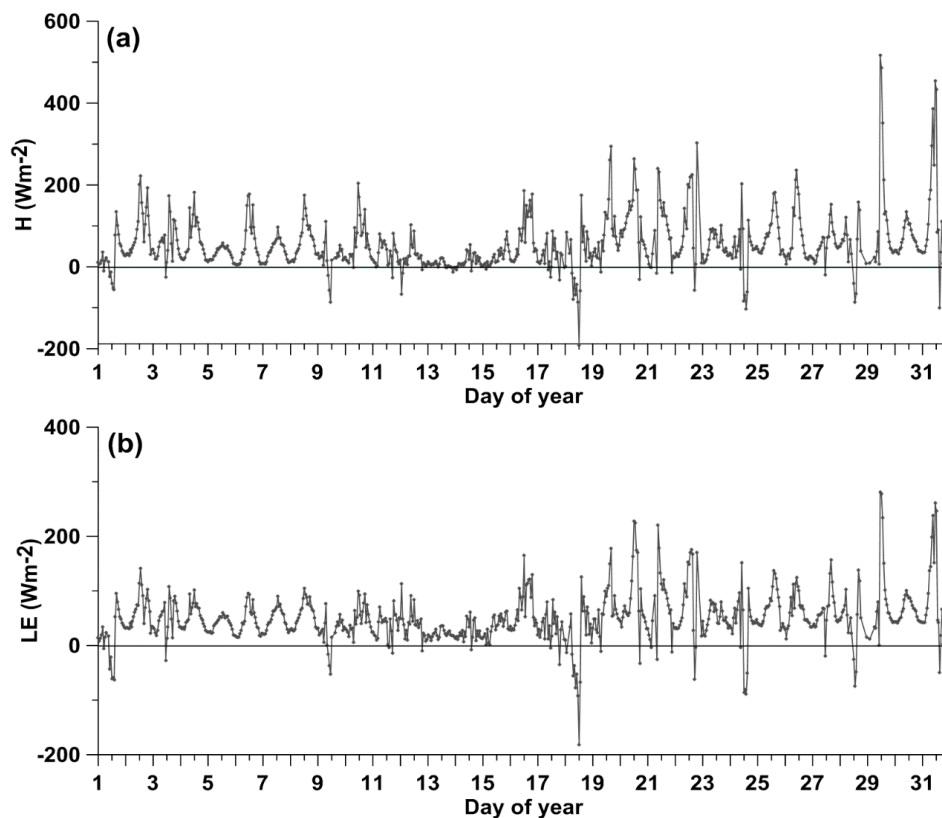


**Figure 10:** Temporal variation of the hourly averaged (a) sensible ( $H$ ) and (b) latent ( $LE$ ) heat fluxes during January 2014 (horizontal straight line indicates 0  $\text{Wm}^{-2}$ ).

The LE also presented a diurnal cycle similar to H (Fig. 10b). LE has 85% of its values between 0 and 100  $\text{Wm}^{-2}$  with most of the values smaller than 50  $\text{Wm}^{-2}$  (Fig. 11b). This is a period of high intensity of the incoming solar radiation (austral summer) and the prevalent positive values of LE may be related to the melting ice sheet that occurs in the region.

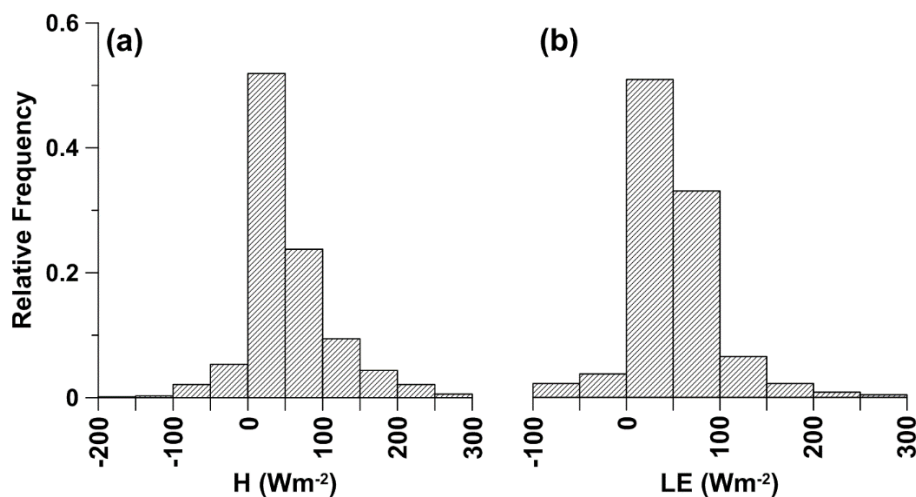


**Figure 11:** Histogram of hourly averaged (a) sensible (H), (b) latent (LE) heat fluxes for January 2014.

The results showed here for heat fluxes agree partially with the study realized by Choi et al. (2008). The authors have studied the net radiation and the turbulent energy exchanges in a non-glaciated coastal area, in King George Island (Sejong Station, located on the north-west edge of the Barton Peninsula), in December 2002 (austral summer). They used the direct method - eddy covariance system - for the estimative of the turbulent fluxes, adopting the same signal convention used here. Choi et al. (2008) have shown that larger net radiation produced larger energy fluxes with a clear influence of cloud cover. The H monthly average was 64  $\text{Wm}^{-2}$  with a large variability due to the snow/ice presence over the surface. The LE values were relatively constant and between 15 and 20  $\text{Wm}^{-2}$ . The sum of H and LE reached approximately 80  $\text{Wm}^{-2}$ , which was an order of magnitude larger than that obtained by Bintanja (1995) at the glaciated areas on the Peninsula Antarctica (-34.8 to 5.6  $\text{Wm}^{-2}$ ). As expected, the turbulent fluxes over non-glaciated areas were more intense than over glaciated area.



Most of the momentum flux has exhibited predominant magnitude of  $10^{-1}$   $\text{Nm}^{-2}$  with approximately 90% of its values smaller than  $0.1 \text{ Nm}^{-2}$  (Fig. 12), agreeing with Stull (1988).

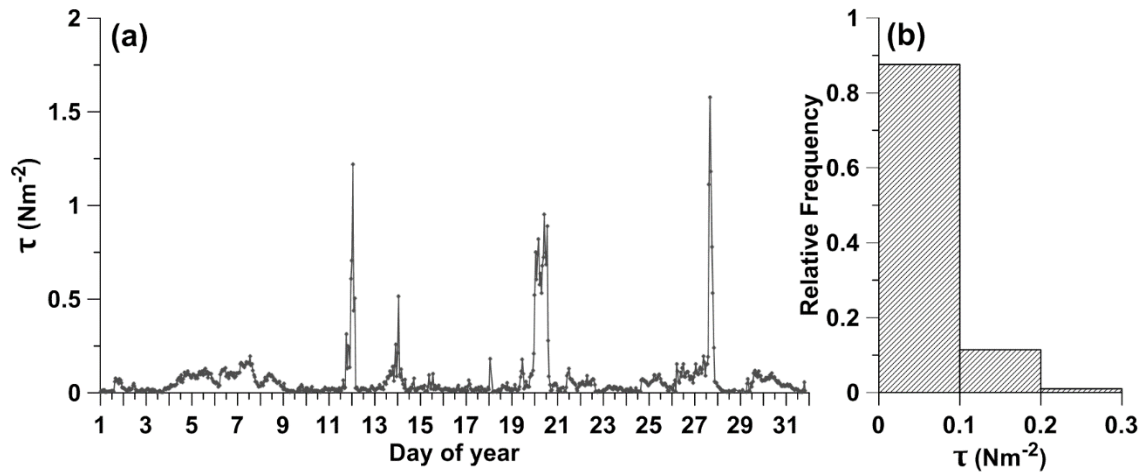


**Figure 12:** Temporal variation of hourly averaged (a) momentum flux ( $\tau$ ) and (b) histogram of hourly averaged  $\tau$  during January 2014.

In the future, the indirect and direct methods will be used to estimate the turbulent fluxes.

### Acknowledgements

The author acknowledges the financial support provided by CAPES and the support of the National Institute of Science and Technology Antarctic Environmental Research (INCT-APA) that receives scientific and financial support from the National Council for Research and Development (CNPq processes: n° 574018/2008-5 and 407137/2013-0) and Carlos Chagas Research Support Foundation of the State of Rio de Janeiro (FAPERJ n° E-16/170.023/2008).

### REFERENCES

- Arya, S. P. S. (2001) Introduction to micrometeorology. 2nd edition, International Geophysics Series, Academic Press, London 420 pp
- Arya, S. P. (2005) Micrometeorology and atmospheric boundary layer. Pure Applied Geophysics 162:1721-1745
- Bintanja R. (1995) The local surface energy balance of the Ecology Glacier, King George Island, Antarctica: measurements and modelling. Antarctic Science 7:315–325

- Braun M., Saurer H., Vogt S., Simões J.C., Goßmann H. (2001) The influence of large-scale circulation on surface energy balance on the King George Island ice cap. *International Journal of Climatology* 21:21-36
- Braun M., Saurer H., Goßmann H. (2004) Climate, energy fluxes and ablation rates on the ice cap of King George Island. *Brazilian Antarctic Research* 4:87-103
- Businger J. A., Wyngaard J. C., Izumi Y., Bradley E. F. (1971) Flux-Profile relationships. *Journal Atmospheric Sciences* 28:181-189
- Choi, T., B. Y. Lee, S. Kim, Y. J. Yoon, H. Lee (2008) Net radiation and turbulent energy exchanges over a non-glaciated coastal area on King George Island during four summer seasons, *Antarctic Science* 20 (1), 99-111.
- Cuxart J., Yagüe C., Morales G., Terradellas E., Orbe J., Calvo J., Fernandez A., Soler M. R., Infante C, Buenestado P., Espinalt A., Joergensen H. E., Rees J. M., Vilà J., Redondo J. M., Cantalapiedra I. R., Conangla L. (2000) Stable atmospheric boundary layer experiment in Spain (SABLES 98): A report. *Boundary Layer Meteorology* 96:337–370
- Dyer, A. J. (1965) The flux-gradient relation for turbulent heat transfer in the lower atmosphere. *Quarterly Journal of the Royal Meteorological Society* 91:151-157
- Dyer, A. J. (1967) The turbulent transport of heat and water vapour in an unstable atmosphere. *Quarterly Journal of the Royal Meteorological Society* 93:501-508
- Dyer, A. J. (1968) An evaluation of eddy flux variation in the atmospheric boundary layer. *Journal Applied Meteorology* 7:845-850
- Dyer, A. J. (1974) A Review of Flux-Profile Relationships. *Boundary Layer Meteorology* 7:363-372
- Fairall C. W., Bradley E. F., Rogers D. P., Edson J. B., Young G. S. (1996) Bulk parameterization of air-sea fluxes for Tropical Ocean-Global Atmosphere Coupled-Ocean Atmosphere Response Experiment. *Journal of Geophysical Research*, 101(2):3747-3764.
- Finnigan J. J., Einaudi F., Fua D. (1984) The interaction between an internal gravity wave and turbulence in the stably-stratified nocturnal boundary layer. *Journal Atmospheric Sciences* 41:2409–2436
- Hicks, B. B. (1976) Wind profile relationships from the Wangara experiments. *Quarterly Journal Royal Meteorology Society* 102:535–551
- Högström, U. (1988) Non-dimensional wind and temperature profiles in the atmospheric surface layer: A re-evaluation, *Boundary Layer Meteorology* 42:55–78
- Högström, U. (1996) Review of some basic characteristics of the atmospheric surface layer. *Boundary Layer Meteorology* 78:215–246
- Jones D. A, Simmonds I. (1993) A climatology of Southern Hemisphere extratropical cyclones. *Climate Dynamics* 9:131–145
- Kramm G., Amaya D. J., Foken T., Mölders N. (2013) Hans A. Panofsky's integral similarity function – at fifty. *Atmospheric and Climate Sciences* 3:581-594
- Laws R. (1990) Science as an Antarctic resource. In: Cook, G. (1990) *The future of Antarctica: exploitation versus preservation*. Manchester University Press, New York City 196pp
- Lee H. N. (1997) Improvement of surface flux calculations in the atmospheric surface layer. *Journal of Applied Meteorology* 36:1416–1423
- Mahrt, L. (1989) Intermittency of atmospheric turbulence. *Journal Atmospheric Sciences* 46:79–95.

- Mahrt L., Sun J, Blumen W., Delany A., McClean G., Oncley S. (1998) Nocturnal boundary-layer regimes. *Boundary Layer Meteorology* 88:255–278
- Martianov V, Rakusa-Suszczewski S. (1989) Ten years of climate observations at the Arctowski and Bellingshausen station (King George Island, South Shetland Islands, Antarctica). *Global Change Regional Research Centres: Scientific Problems and Concept Developments*. Warsaw-Jablonna, IGBP IASA UNESCO PAS Seminar, Birkenmajer A. Institute of Geography and Spatial Organization: Warsaw, Poland, 80–87
- Monin A. S., Obukhov A. M. (1954) Basic Laws of turbulent mixing in the ground layer of the atmosphere. *Akad. Nauk. SSSR Geofiz. Inst. Tr.* 151:163-187
- Moura R.B. (2009) Estudo taxonômico dos Holothuroidea (Echinodermata) das Ilhas Shetland do Sul e do Estreito de Bransfield, Antártica. Master Dissertation, Museu Nacional, Universidade Federal do Rio de Janeiro, Rio de Janeiro, 111 pp
- Parish T. R. (1983) The influence of the Antarctica Peninsula on the wind field over the western Weddell Sea. *Journal of Geophysical Research*, 88:2684-2692
- Paulson C. A. (1970) The Mathematical Representation of Wind Speed and Temperature Profiles in the Unstable Atmospheric Surface Layer. *Journal Applied Meteorology* 9:857–861
- Poulos G. S., Blumen W., Fritts D. C., Lundquist J. K., Sun J., Burns S. P., Nappo C., Banta R., Newsom R., Cuxart J., Terradellas E., Balsley B., Jensen M. (2002) CASES-99: A comprehensive investigation of the stable nocturnal boundary layer. *Bulletin American Meteorology Society* 83:555–581
- Rachlewicz G. (1997) Mid-winter thawing in the vicinity of Arctowski station, King George Island. *Pol Polar Res* 18:15–24
- Rakusa-Suszczewski S. (1993) The maritime Antarctic coastal ecosystem of Admiralty Bay. Warsaw: Polish Academy of Sciences, 216 pp
- Schwerdtfeger W. (1984) *Weather and Climate of the Antarctic*. Elsevier, Amsterdam.
- Sharan M., Rama Krishna T. V. B. P. S., Aditi (2003) On the bulk Richardson number and flux–profile relations in an atmospheric surface layer under weak wind stable conditions. *Atmos. Environ.* 37:3681–3691
- Smith R.C., Stammerjohn S.E., Baker K.S. (1996) Surface air temperature variations in the western Antarctic Peninsula region. *Antarctic Research Series* 70:105–121
- Stull, R. B. (1988) *An introduction to boundary layer meteorology*. Kluwer Academic Press, Dordrecht 666pp
- Webb, E. K. (1970) Profile relationships: The log-linear range and extension to strong stability, *Quart. J. Roy. Meteorol. Soc.* 96:67–90
- Wen J., Kang J., Han J., Xie Z., Liu L., Wang D. (1998) Glaciological studies on King George Island ice cap, South Shetland Islands, Antarctica. *Annals of Glaciology* 27:105–109
- WGASF (2000) Intercomparison and validation of ocean-atmosphere energy flux fields. Final report of Joint WCRP/SCOR Working Group on Air-Sea fluxes (SCOR working group 110)
- Yagüe C., Cano J. L. (1994) The influence of stratification on heat and momentum turbulent transfer in Antarctica, *Boundary Layer Meteorology* 69:123–136

- Yagüe C. Viana S., Maqueda G., Redondo J. M. (2006) Influence of stability on the flux-profile relationships for Wind speed,  $\Phi_m$ , and temperature  $\Phi_h$ , for the stable atmospheric boundary layer. *Nonlinear Processes in Geophysics* 13:185-203
- Zilitinkevich S. S., Chailikov D. V. (1968) Determining the universal wind velocity and temperature profiles in the atmospheric boundary layer. *Izvestiya, Atmos. Ocean. Phys.* 4:165–170
- Zilitinkevich S. S., Elperin T., Kleerorin N., Rogachevskii I. (2007) Energy – and flux-budget (EFB) turbulence closure model for stably stratified flows. Part I: steady-state, homogenous regimes. *Boundary Layer Meteorology* 125:167-191
- Zilitinkevich S. S., Esau I. N. (2007) Similarity theory and calculation of turbulent fluxes at the surface for the stably stratified atmospheric boundary layer. *Boundary Layer Meteorology* 125:193-205